Changes in Cell Size and Dimension Characterized by Crystal Violet Staining and Simple ImageJ Analysis

Somying Patntirapong[1]*, Pattranith Charoensukpatana[2], Thitaree Thaksinawong[2]

1. Thammasat University Research Unit in Dental and Bone Substitute Biomaterials, Faculty of Dentistry, Thammasat University, Pathumthani, Thailand.
2. Faculty of Dentistry, Thammasat University, Pathumthani, Thailand.

Abstract

Bisphosphonate (BP) and geranylgeraniol (GGOH) are known drug/reagent affecting osteoblast shape and dimensions. Digital image analysis such as ImageJ can detect changes in cell dimensions. Commonly, fluorescence staining, a high-cost dye, is used for staining cells. Therefore, this study was attempted to investigate dimensional changes in cells stained with a simple and low-cost dye and measured by ImageJ analysis.

Pre-osteoblast, MC3T3, cells were incubated with alendronate (ALN) and GGOH. Cells were stained with crystal violet and were recorded for quantitative measurements via ImageJ. The measurement procedure was defined to perform cell segmentation. Cell area, number, dimensions, and aspect ratio were measured.

Crystal violet staining method exhibited similar results to fluorescence staining method in terms of cell area and aspect ratio. ImageJ distinguished the changes in cell numbers and cell sizes after treating with ALN and GGOH. Furthermore, the result obtaining from the automated ImageJ method was comparable to that of the manual ImageJ method in terms of aspect ratio.

The staining and analyzing technique detected pre-osteoblast dimensional changes after ALN and GGOH treatments. It was practical and easy to use. It could be an alternative method for screening of cell changes after drug treatment.

Experimental article (J Int Dent Med Res 2022; 15(1): 1-6)

Keywords: Cell dimension, crystal violet staining, ImageJ, bisphosphonate, geranylgeraniol.

Received date: 21 January 2022 **Accept date:** 17 February 2022

Introduction

In biomedical study, there is a growing demand for a screening system that is simple, precise, capable of rapidly building data, and versatile for a variety of applications. Digital image analysis has been widely developed and is used in various biomedical applications because of its positive impact on altering qualitative data to quantitative data.[1-4] One of the most commonly used digital analysis software is ImageJ. It is a reliable and free downloadable software with various functions.[5]

Corresponding author:
Associate Professor Somying Patntirapong, DDS, DMSc
Thammasat University Research Unit in Dental and Bone Substitute Biomaterials,
Faculty of Dentistry, Thammasat University, Rangsit campus
99 Moo 18 Pahonyothin Rd., Klong Luang,
Pathumthani, 12120, Thailand.
E-mail: p_somying@hotmail.com; psomying@tu.ac.th

An example of the drugs that is related to the dental field is BP. This drug is prescribed to prevent excessive bone resorption.[6] However, it is found to relate to a condition called medication-related osteonecrosis of the jaw since 2003.[7-9] Therefore, the studies of BP are extensively examined.[10-14] In order to screen and rapidly obtain data, *in vitro* cell culture-based screening test has been emerging in the pharmaceutical industry. This system can be performed rapidly and quantified high volume of information, which is later applied in *in vivo* and clinical tests.[15]

In this study, we aimed to exploit a simple method to evaluate the changes in cell size and dimension. ALN (a nitrogen-containing BP) and GGOH were utilized since the drug/reagent are previously shown to alter cell morphology and cell size.[2, 16] Crystal violet dye was used instead of high-priced fluorescence dye because it is a simple as well as economical staining technique and can be visualized under a regular light microscopy. The processing method of ImageJ

analysis was modified to investigate cell dimensional changes. By using this procedure, the changes of cells could promptly be identified. This would be a potential tool for predicting or screening responses of cells to *drug treatment and/or other stimuli, which could be applied* in cytopathology and *in vitro* studies.

Materials and methods

Murine osteoblast precursors, MC3T3 cells were plated at a density of 8,000 cells/cm^2 in α-minimum essential medium (Gibco) containing 10% fetal bovine serum and 1% penicillin/streptomycin at 37°C and 5% CO_2 humidified atmosphere. MC3T3 cells were treated with ALN at 10 μM (A10) and GGOH at 10, 50, and 100 μM (G10, G50, and G100) for 3 days. Cell with no treatment (A0G0) served as a negative control and cell treated with 10 μM ALN (A10G0) served as a positive control.

After 3-day incubation, cells were fixed with 4% paraformaldehyde for 15 minutes at room temperature. Fixed cells were stained with crystal violet (Life Science Dynamic Division, Arnaporn Co., LTD) for 5 min, and rinsed carefully. Cell appearance was examined under a light microscope (Nikon Eclipse TS100) at 200x magnification. Eight random fields from two wells were recorded using a Nikon Digital sight DS-L2. Nine to ninety cells were scored for each field. For quantitative analyses, ImageJ software version 1.52a Java 1.8.0 (National Institute of Health) was performed. The following parameters were analyzed: %area, cell number, cell size (area; μm^2), cell length and width (μm), and aspect ratio. Rhodamine phalloidin staining was performed as described in Patntirapong, 2021.[2] This method served as a conventional staining method.

The scale was first set using “Analyze > Set Scale” command. A micrometer unit was fixed by choosing the “Global” button in order that every image had equal scale for measurement. Original images were processed by two identifications: automated and manual detections. The background of images was optionally eliminated by picking the “Process > Subtract Background” function. This option flattened uneven background and allowed the processing of images with bright background and dark objects. Images were converted to grayscale by running “Image > Type > 8-bit”. The images were processed with “Image > Adjust > Auto Threshold” commands. “Huang” and “SetThreshold instead of Threshold” were picked. The focused area then displayed in red color. Because some cells attached on the well plate as clusters, the following functions were applied: “Process > Binary > Make Binary” and “Process > Binary > Watershed”. The objects of interest were changed to black objects over white background. The clustered cells were segmented from one another. By these steps, the identified cells were ready for analyzing. For automated detection, the parameters were characterized by “Analyze > Analyze Particles" function. It should be noted that the particles smaller than 200 μm^2 were excluded. For %area, "Analyze > Measure" function was selected instead of “Analyze Particles” function.

For calculating the length and width of the cells, an extra step was applied. The “Straight” and then “Analyze > Measure” commands were used manually to measure major and minor axis of each single cell. Major/minor axis of each cell was later calculated for aspect ratio.

Normality test was performed by Shapiro-Wilk test using GraphPad Prism version 5 (GraphPad software). Data were then analyzed by One-way analysis of variance followed by Dunnett multiple comparison test and unpaired t-test. Data were expressed as means ± SD. Significance was assigned as $^*p < 0.05$, $^{**}p < 0.01$, and $^{***}p < 0.001$ vs A0G0. Significance was assigned as $^{\phi}p < 0.05$, $^{\phi\phi}p < 0.01$, and $^{\phi\phi\phi}p < 0.001$ vs A10G0.

Results

By visual inspection, cells in each treatment condition seemed to show different cell shapes, dimensions, and spreading. Cells were distributed on the well plate as clusters or a single cell. MC3T3 cells in untreated condition (A0G0) exhibited polygonal to cuboidal shapes. A10G0 cells demonstrated fusiform and round shapes. Addition of G50 and G100 to A10 cells were able to alter A10 cells to cuboidal shape. Cell shape in this condition appeared to be more homogeneity than in A0G0 and A10G0 (Figure 1).

Next, the qualitative data were converted into quantitative data. The modified staining method (crystal violet) was initially compared to the conventional staining method (rhodamine phalloidin) using A0G0 condition. The workflow of

system analysis for crystal violet staining was shown in Figure 2A-F. The representative schemes for rhodamine phalloidin were presented in Figure 2G-H. The area per cell and aspect ratio (AR) of both staining were assessed. The measurements of crystal violet staining were comparable to those of rhodamine phalloidin staining [Figure 2I and J]. The average area per cell for rhodamine phalloidin and crystal violet was 789 ± 724 and 802 ± 554 μm^2, respectively (Figure 2I). The average AR was 1.6 ± 0.45 for rhodamine phalloidin and 1.61 ± 0.46 for crystal violet (Figure 2J). The similarity of these data suggested the potential use of crystal violet.

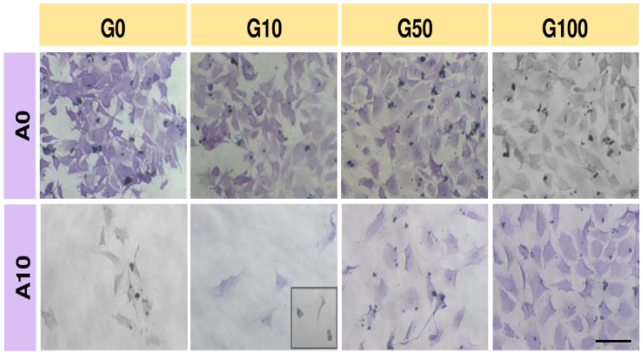

Figure 1. Crystal violet-stained images. MC3T3 cells were treated with ALN and GGOH at different concentrations for 3 days. Representative images showed cells stained positive to crystal violet. The changes in cell morphology were monitored by light microscopy. Inset illustrated round-shaped cells from another view. Scale bar = 100 µm.

We later applied crystal violet staining and an automated function of ImageJ method to cells treated with ALN and GGOH. The %area coverage, cell number, and cell size were determined. The %area coverage is quantified using an Area Fraction output of ImageJ in order to demonstrate cell growth.[4, 17] The difference of %area was distinguished among groups. A0G0 covered the well area more than 40%. No significant difference was observed in the addition of GGOH. Cells subjected to treatments with A10 occupied less than 5% area. In the presence of GGOH, increases in the area coverage were monitored (Figure 3A).

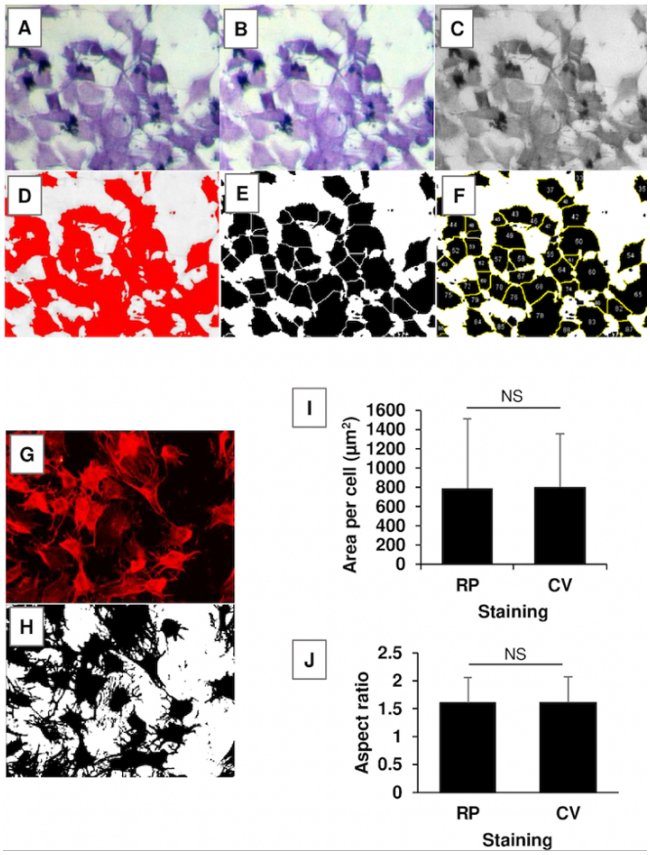

Figure 2. ImageJ processing and comparison between crystal violet and rhodamine phalloidin staining methods. The workflow of crystal violet-stained cell segmentation was demonstrated as followed: (A) Original image was obtained. (B) The image background was subtracted. (C) The image was converted to grayscale. (D) Thresholding was applied to the image. (E) Each cell was segmented by watershed function. (F) ImageJ labeled each cell separately. The representative schemes of rhodamine phalloidin-stained cells are presented in (G) Original image and (H) Thresholding image. (I) Area per cell graph. (J) Aspect ratio graph. RP; rhodamine phalloidin, CV; crystal violet, NS; not significant.

The cell segmentation procedure could distinguish individual cells from background and the adjacent cells, despite these cells being assembled closely together (Figure 2E). The software was able to mark each single cell in the resulting images (Figure 2F), hence, granting an automatic cell count. A0G0 were approximately 75 cells per field. A10G0 were significantly lost from the culture plate and had been estimated to be around 9 cells. The addition of G100 increased the number of cells on the well surface (Figure 3B).

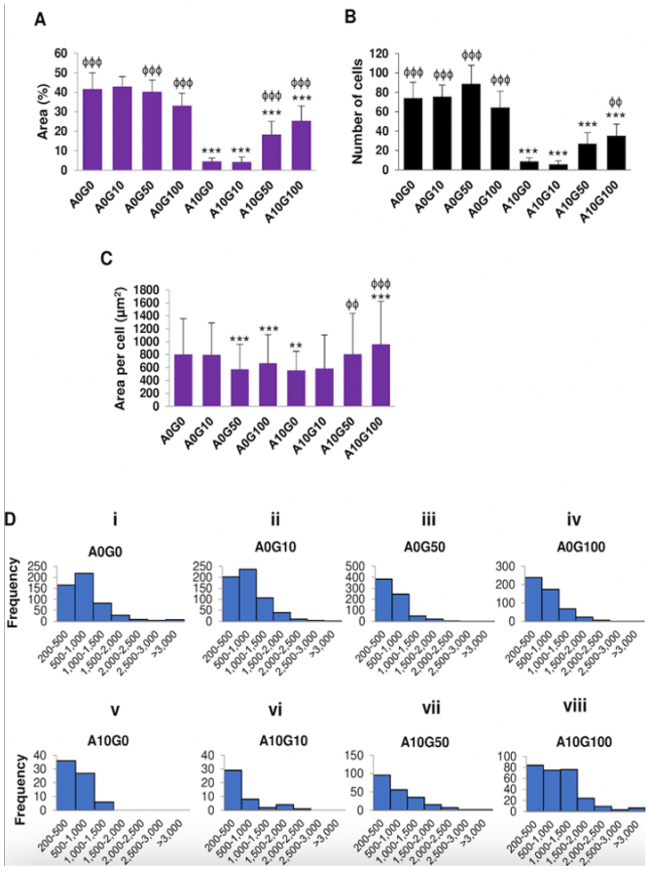

Figure 3. Calculation of pre-osteoblast cell area by automated procedure. (A) Area fraction. (B) Number of cells. (C) Area per cell (μm^2). (D) Distribution of cell size.

Figure 3C demonstrated the difference of average single cell spreading area. Calculation of the cell area showed a significant reduction of cell size in A10G0 group compared with A0G0. The addition of G50 and G100 to A10-treated cells markedly increased in cell size (Figure 3C). The cell size was later established in histogram to present the distribution of the area per cell (Figure 3D). In A0G0, the distribution frequency of cell area mostly fell into 500-1,000 μm followed by 200-500 μm range (Figure 3Di). The addition of G50 and G100 to A0 cells as well as A10 shifted the distribution of cells to a smaller size range (Figure 3Diii-Dv). Cells in the A10G0 group mostly contain 200-500 μm size range with the frequency at around 35. Cell size larger than 1,500 μm was not seen (Figure 3Dv). Cell size larger than 1,500 was speculated after GGOH treatment to A10 cells (Figure 3Dvi-Dviii). Cells in A10G100 treatment showed the equal distribution of cell size among the 200-500, 500-1,000, and 1,000-1,500 μm range [Figure 3Dviii].

These results indicated an ability of the technique used in this study to characterize cells in different conditions.

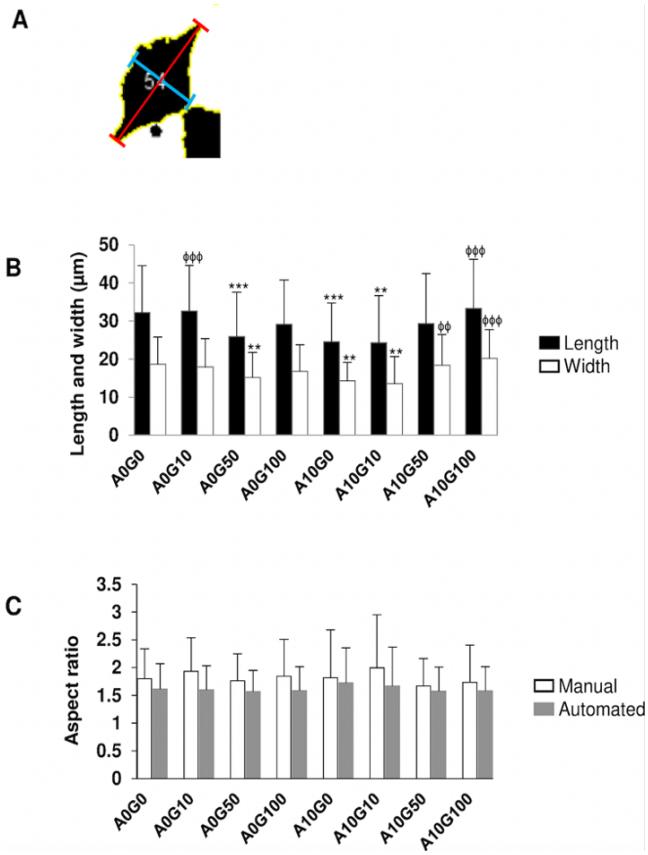

Figure 4. Estimation of cell dimensions. (A) After cell segmentation, length (red line) and width (blue line) were manually measured. (B) Length and width measured by manual procedure. (C) Quantification of aspect ratio calculated by automated and manual methods.

Cell dimensions, length and width, were measured. The alteration could be assessed by manual and automated quantifications. The manual measurement had been done to assess the length and width of each cell (Figure 4A). Cells incubated with A10 were significantly smaller in length and width than A0 cells. A10G100 notably increased cell dimensions compared with A10G0 (Figure 4B). AR, which is major axis/minor axis, was calculated. AR determined manually was compared with AR calculated automatedly. No significant difference was observed between automated versus manual identifications (Figure 4C), verifying the comparability of the automated method to the manual method

Discussion

ImageJ is now being used for various imaging applications, which can read most of the common formats used in the field of biomedical imaging.[5] The examples of ImageJ use include examination of immunohistological staining, analysis of fluorescence staining, evaluation of mitochondrial network morphology, and interpretation of alizarin red and alkaline phosphatase staining, and etc.[1-4] Here, we demonstrated another application of ImageJ that could be used in the research field using crystal violet staining.

For morphometric analysis of cells, cell cytoskeleton is usually stained with fluorescence dye and cell size is examined using fluorescence/confocal microscopy.[2, 18] By utilizing the fluorescence method, previous study reports the changes in osteoblast shape treated with ALN and GGOH.[2] In this study, cell dimensional change was characterized by different staining system and a modified automated procedure. Crystal violet staining is a simple and affordable staining technique. It is one of the most common techniques used in staining adherent cells.[11, 19] The dye binds to proteins and DNA in cells[20], marking cell boundary and cell morphology. Although this staining technique is not new, however, to our knowledge application of this dye to pre-osteoblast together with utilizing automated ImageJ analysis has not been performed. The finding showed that cells stained with crystal violet dye could be successfully segmented and quantified by ImageJ. The technique described in this study was able to convert qualitative to quantitative data. The changes in cell size after ALN and GGOH treatments also demonstrated the same trend as reported by Patntirapong, 2021[2], implying the practicality of this modified method. This technique could be applied for screening cell dimensions and growth under various drug conditions.

The ImageJ software distinguished the crystal violet staining from the background. The watershed function segmented the clustered cells separating one cell from another cell, resulting in the ability to detect a single cell area. However, there is a limitation using the software. The automated threshold function requires a fair quality image for analysis. In case of low-quality image, the contrast and brightness functions can be pre-processed to make the cells more distinguishable from the background before threshold function is applied.[21]

Manual identification method is widely accepted in biological and medical image analysis. Nonetheless, the method requires strenuous task to obtain the data compared to automated measurement. The automated method can analyze a quantity of images with less time for researchers.[21] Furthermore, this procedure is more scientifically objective method than manual image analysis and can be reproduced[22], thus avoiding inter-observer variability. With an easily understandable procedure and advantage, this modified method could be used as an alternative option in the research field to obtain data.

Conclusions

The modified method, crystal violet staining and an adapted ImageJ procedure, could detect the changes in pre-osteoblast dimensions after ALN and GGOH treatments. This method is easy to function and can analyze a number of images without script writing to execute the program. This method might be useful for other applications in the field of biology and medical sciences, e.g. screening of cell morphological changes after drug treatment.

Acknowledgements

This work was supported by Thammasat University Research Unit in Dental and Bone Substitute Biomaterials, Thammasat University, Thailand. We also thank Nareerat Korjai, Monticha Matchimapiro, Paphada Sungkaruk, Yauwaluk Suthamporn for the preparation of art work.

The funding for this study was partially granted by Faculty of Dentistry, Thammasat University.

Declaration of Interest

The authors declare that they have no conflict of interest.

References

1. Yoon JH, Li M, Basile JR, Lin YL. Computer-assisted analysis of immunohistological parameters in oral giant cell granulomas. Oral Dis 2019;25(3):796-802.

2. Patntirapong S, Korjai N, Matchimapiro M, Sungkaruk P, Suthamporn Y. Geranylgeraniol reverses alendronate-induced MC3T3 cell cytotoxicity and alteration of osteoblast function via cell cytoskeletal maintenance. J Oral Pathol Med 2021;50(2):191-9.
3. Valente AJ, Maddalena LA, Robb EL, Moradi F, Stuart JA. A simple ImageJ macro tool for analyzing mitochondrial network morphology in mammalian cell culture. Acta Histochem 2017;119(3):315-26.
4. Patntirapong S, Chanruangvanit C, Lavanrattanakul K, Satravaha Y. Assessment of bisphosphonate treated-osteoblast behaviors by conventional assays and a simple digital image analysis. Acta Histochem 2021;123(1):151659.
5. Abramoff MD, Magalhaes PJ, Ram SJ. Image processing with ImageJ. Biophotonics International 2004;11:36-42.
6. Russell RG, Watts NB, Ebetino FH, Rogers MJ. Mechanisms of action of bisphosphonates: similarities and differences and their potential influence on clinical efficacy. Osteoporos Int 2008;19(6):733-59.
7. Marx RE. Pamidronate (Aredia) and zoledronate (Zometa) induced avascular necrosis of the jaws: a growing epidemic. J Oral Maxillofac Surg 2003;61(9):1115-7.
8. Ruggiero SL, Dodson TB, Fantasia J, et al. American Association of Oral and Maxillofacial Surgeons position paper on medication-related osteonecrosis of the jaw-2014 update. J Oral Maxillofac Surg 2014;72(10):1938-56.
9. Kilic E, Gonen ZB, Alkan A. Osteonecrosis related to oral bisphosphonate usage: case report and review of treatment strategies. J Int Dent Med Res 2012;5(1):45-8.
10. Odvina CV, Zerwekh JE, Rao DS, et al. Severely suppressed bone turnover: a potential complication of alendronate therapy. J Clin Endocrinol Metab 2005;90(3):1294-301.
11. Patntirapong S, Singhatanadgit W, Chanruangvanit C, Lavanrattanakul K, Satravaha Y. Zoledronic acid suppresses mineralization through direct cytotoxicity and osteoblast differentiation inhibition. J Oral Pathol Med 2012;41:713–720.
12. Orriss IR, Key ML, Colston KW, Arnett TR. Inhibition of osteoblast function in vitro by aminobisphosphonates. J Cell Biochem 2009;106(1):109-18.
13. Burr DB, Allen MR. Mandibular necrosis in beagle dogs treated with bisphosphonates. Orthod Craniofac Res 2009;12(3):221-8.
14. Venkataramana V, Rajasigamani K, Madhavan N, et al. The effect of bisphosphonate [Pamidronate] on orthodontic tooth movement in Newzealand albino rabbits. J Int Dent Med Res 2012;5(3):136-42.
15. Kitaeva KV, Rutland CS, Rizvanov AA, Solovyeva VV. Cell Culture Based in vitro Test Systems for Anticancer Drug Screening. Front Bioeng Biotechnol 2020;8:322.
16. Kazmers NH, Ma SA, Yoshida T, Stern PH. Rho GTPase signaling and PTH 3-34, but not PTH 1-34, maintain the actin cytoskeleton and antagonize bisphosphonate effects in mouse osteoblastic MC3T3-E1 cells. Bone 2009;45(1):52-60.
17. Busschots S, O'Toole S, O'Leary JJ, Stordal B. Non-invasive and non-destructive measurements of confluence in cultured adherent cell lines. MethodsX 2015;2:8-13.
18. Elosegui-Artola A, Jorge-Penas A, Moreno-Arotzena O, et al. Image analysis for the quantitative comparison of stress fibers and focal adhesions. PLoS One 2014;9(9):e107393.
19. Habibi H, Suzuki A, Hayashi K, et al. Expression and function of fibroblast growth factor 1 in the hypertrophied ligamentum flavum of lumbar spinal stenosis. J Orthop Sci 2021; S0949-2658.
20. Feoktistova M, Geserick P, Leverkus M. Crystal Violet Assay for Determining Viability of Cultured Cells. Cold Spring Harb Protoc 2016;2016(4):pdb prot087379.
21. Venter C, Niesler CU. Rapid quantification of cellular proliferation and migration using ImageJ. Biotechniques 2019;66(2):99-102.
22. Georg M, Fernandez-Cabada T, Bourguignon N, et al. Development of image analysis software for quantification of viable cells in microchips. PLoS One 2018;13(3):e0193605.